

Cyclic stress ratio definitions under generalized seismic loading paths

Prasanna Rousseau¹ and Siva Sivathayalan²

¹School of Civil and Environmental Engineering Indian Institute of Technology. Mandi Mandi, Himachal Pradesh, India

²Civil and Environmental Engineering Carleton University Ottawa, ON, Canada

¹prasanna@iitmandi.ac.in and ²Siva.Sivathayalan@carleton.ca

Abstract: Liquefaction susceptibility of soils is conventionally assessed by comparing the cyclic stress ratio (CSR) against the cyclic resistance ratio (CRR) of the soil. CSR quantifies the seismic demand on the soil layer, while CRR represents the capacity of the soil to withstand the shaking for a given earthquake magnitude. Both CSR and CRR represent normalized forms of shear stress to effective confining stress, but the lack of consistency among the quantities selected to represent the shear stress, and the effective confining stress has led to contradictions in the literature, and made comparisons difficult. The commonly highlighted differences between the cyclic triaxial (CRR_{TX}) and cyclic simple shear (CRR_{SS}) resistance is partly attributable to the discrepancies in the CSR definition. Typically, geotechnical practice relies on 2D based formulations presuming that dynamic loading during earthquakes occurs primarily due to vertically propagating shear waves. Wave propagation analysis reveal that this approach is an oversimplification applicable to perfectly horizontal layering and homogeneous soil strata. The inevitable nature of heterogeneity in natural soils, and inclined soils strata result in complicated seismic wave propagation. These results show that in reality the in situ dynamic loading would consist of cyclic shear stresses and cyclic normal stresses due to various geological phenomena. This raises a concern of the validity of the current CSR determination procedures, and their applicability under generalized 3D loading conditions. Variations in CSR definitions affect the Factor of Safety (FOS) against liquefaction, which in turn impacts critical decisions regarding site selection and ground improvement techniques, potentially increasing project costs. By exploring the intricacies of wave propagation in heterogeneous soil strata, this study aims to alert the profession to the challenges in using simple formulations to quantify CSR and CRR.

Keywords: Soil Liquefaction, Seismic waves, Cyclic resistance, Cyclic stress ratio, loading paths.

Introduction

An assessment of the liquefaction potential of soils is essential for proper planning and design of any major infrastructural facility. In conventional practice, the liquefaction susceptibility of soils is evaluated by comparing

the cyclic stress ratio (CSR) with the cyclic resistance ratio (CRR) of the soil [1]. CSR and CRR represent normalized forms of shear stress to effective confining stress, and CSR represents the seismic demand on the soil layer,

whereas CRR represents the capacity of the soil to resist liquefaction given a specific earthquake magnitude.

The basic understanding of cyclic liquefaction potential and the effects of various factors controlling it have been derived from controlled laboratory experiments. Cyclic triaxial tests (CTX), primarily, and cyclic simple shear (CSS) to a lesser extent have typically been employed in this line of research. CTX is an axisymmetric test, and CSS plane strain, and thus the findings are applicable only to such stress states. Cyclic torsional hollow-cylinder shear tests (CHC) permit an assessment of the behavior under generalized 3D loading conditions, but have been rare. The CSR and CRR in these experiments have been defined based on the parameters measured/available in each type of test.

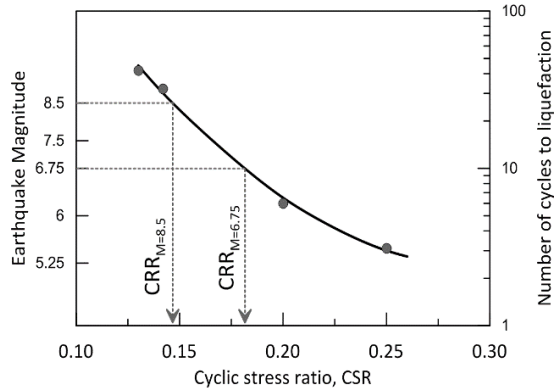


Figure 1: Determination of CRR from the cyclic resistance curve

A cyclic resistance curve showing the variation of CSR vs number of cycles to liquefaction is used to determine the CRR corresponding to liquefaction for a given number of cycles (or for a specific earthquake magnitude), as illustrated in Figure 1. Design practice is typically based

on empirical relationships [2], except in critical projects where both empirical and laboratory assessments are considered. In-situ assessments using empirical approaches characterize CSR as the ratio of the cyclic shear stress on the horizontal plane (τ_{cy}) to the effective vertical overburden stress (σ'_{v0}), yielding

$$\text{CSR}_{\text{IS}} = \frac{\tau_{cy}}{\sigma'_{v0}}. \quad (1)$$

In the laboratory, the CSR is defined in different ways depending on the loading mode and the parameters measured in the test. It is a ratio, where the numerator is a measure of the maximum shear stress (τ_{max}), and it is logical to use the maximum amplitude of the cyclic shear stress, $\frac{\sigma_{d,cy}}{2}$. The denominator is a measure of the confining stress. Early CTX tests used the effective cell pressure σ'_c to denote the confining stress, yielding

$$\text{CSR}_{\text{TX}} = \frac{\sigma_{d,cy}}{2\sigma'_c}. \quad (2)$$

This was broadly accepted and perfectly fine at the time since the CTX tests were generally conducted on hydrostatically consolidated specimens, and thus $\sigma'_c = \sigma'_{vc} = \sigma'_{hc}$.

Cyclic simple shear (CSS) tests are known to closely simulate in situ loading conditions due to vertically propagating shear waves. Therefore, in a CSS test, CSR is defined as

$$\text{CSR} = \frac{\tau_{h,cy}}{\sigma'_{vc}}, \quad (3)$$

which closely matches the definition of CSR_{IS} noted previously.

However, the realization that initial static shear stresses may significantly influence cyclic resistance, and the fact that in-situ stress states

are rarely hydrostatic, led to the introduction of CTX tests on anisotropically consolidated specimens. Despite this, CSR was still calculated in the same way even though $\sigma'_{vc} \neq \sigma'_{hc}$ in these triaxial tests. This approach was guided by the practice of normalizing shear strength in monotonic tests by the minor principal stress to obtain the strength ratio. Initial static shear stresses in simple shear are represented by a shear stress on the horizontal plane ($\tau_{h,st}$) during consolidation. Here, the major principal stress is no longer vertical, and $\sigma'_{vc} \neq \sigma'_{1c}$, but again the CSR is calculated using τ_{cy}/σ'_{vc} in these simple shear tests. Under a 3D stress state, CSR is defined as $\sigma_{d,cy}/2\sigma'_{mc}$, which is typically used in CHC testing. Alternate formulations that use the second invariant (J_2) of the deviatoric stress matrix have also been recommended under 3D loading conditions [3, 4].

In summary, the definition of CSR across different loading modes lacks consistency. The maximum cyclic shear stress is normalized by the effective minor principal stress, effective mean normal stress, or effective vertical stress, which in some cases is equal to the effective major principal stress (σ'_{1c}), and at other times is not. Clearly, the normalization parameter is of paramount importance. Although σ'_{3c} has been widely used to determine strength ratios in the past, recent data in the literature suggests that normalization with respect to σ'_{1c} yields more consistent responses under generalized loading [5,6]. A series of tests were conducted at the same effective mean normal stress, but with different σ'_{1c} and σ'_{3c} to represent various levels of initial static shear. The direction of the major principal stress α_σ was also varied

from 0° to 90° to represent generalized 3D loading conditions.

Figure 2(a) shows the variation of the shear strength at steady or quasi-steady state normalized by σ'_{3c} , and Figure 2(b) the shear strength normalized by σ'_{1c} . The wide scatter present in Figure 2(a) essentially disappears and the data falls within a very narrow band in Figure 2(b).

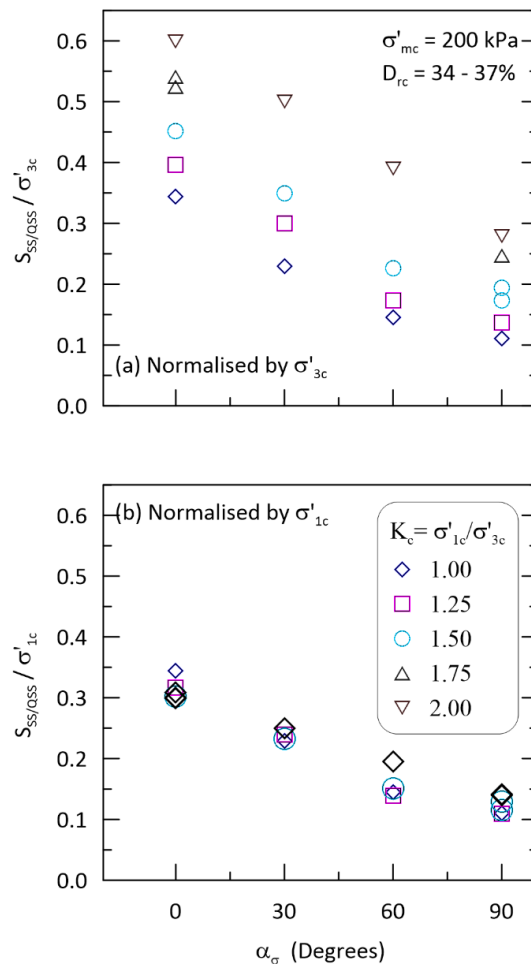


Figure 2: Influence of the normalizing parameter on the undrained strength ratio characterization (modified after Sivathayalan [5])

This finding indicates that normalization using effective major principal stress should be preferred as it yields a more consistent strength

ratio. The main objective of the various approaches to CSR (Cyclic Stress Ratio) definition has been to quantify the shear stress induced due to the propagation of shear waves (S-waves) during seismic shaking. The basis for considering only the propagation of pure S-waves during an earthquake for liquefaction triggering analysis is the assumption of perfectly horizontal and homogeneous soil strata. This assumption is overly simplistic because the actual in-situ soil media is highly heterogeneous, and the plane of stratification is not horizontal, making the actual propagation of seismic waves very complex in the soil strata [7].

As a result of the complex interaction of seismic waves with the soil strata, seismic waves are reflected and refracted into waves of different nature and characteristics. This interaction depends on the differences in seismic impedance between soil layers or bedrock and the incidence angle of the seismic waves. The reflected and refracted waves are multiple-phase waves and may consist of both compression wave (P-wave) and shear wave (S-wave) components. This indicates that during an earthquake, the soil element will inevitably be subjected to complex loading paths involving the simultaneous action of both normal and shear stresses. This combination affects the variation of τ_{\max} , which in turn affects the definition of CSR. Generally, in laboratory experiments, a sinusoidal variation of τ_{\max} is considered by assuming a sign convention for τ_{\max} , simplifying the definition of CSR. However, the variation of τ_{\max} with the assumption of a sign convention becomes complicated for complex loading paths. The current method of defining CSR does not account for these complex loading paths and

the resulting variation in shear stresses.

The definition of CSR varies based on the loading mode and stress state. Establishing a unique relationship for CSR is crucial, particularly in the context of laboratory testing, as the CRR (Cyclic Resistance Ratio) - essentially the CSR required to liquefy soil under a given number of loading cycles - is derived from it. This variability in CSR definitions impacts the determination of the factor of safety (FOS) against liquefaction. Even minor changes in the factor of safety can lead to critical decisions, such as the selection of a construction site and the implementation of ground improvement techniques, which can significantly increase the cost of infrastructural projects.

Previous studies have noted the differences in the CRR measured in CTX and CSS tests [8-10] and attributed these differences to their varying states of consolidation stress. However, these studies did not consider the effects of loading mode or the complexities of seismic wave propagation. Some research has addressed the definition of CSR under bi-directional simple shear loading [11], but this is limited to simulating the propagation of S-waves. Only a few studies have explored the complexities involved in seismic wave propagation, specifically the complex loading paths resulting from the combined action of both P-waves and S-waves [7], and how this intricate interaction impacts the definition of CSR [3,12]. In keeping this in mind, this paper aims to discuss the complex propagation of seismic waves in soil strata and how it results in intricate seismic loading paths. The variation of τ_{\max} under these complex generalized loading

paths and its implications for the estimation of CSR are examined. Gaining a deeper understanding of the complex variation of shear stresses under generalized 3D dynamic loading paths is essential for advancing the methods of assessing soil liquefaction potential.

Propagation of Seismic Waves

Traditional one-dimensional (1D) shake models and two-dimensional (2D) horizontal numerical models have been widely used to analyze seismic wave propagation and estimate shear stresses on the horizontal plane to determine the CSR. In typical geotechnical analysis, the soil profile is modeled as a series of horizontal layers, and the seismic waves are assumed to propagate vertically, which simplifies the problem into 1D wave propagation. The primary objective of these models is to simulate the propagation of pure shear waves (S-waves). However, in reality, during seismic loading, the soil will be subjected to the combined action of both compression waves (P-waves) and shear waves (S-waves). This limitation means that these models fail to capture the complex interactions between seismic waves and soil layers. Similarly, 2D horizontal models assume horizontal layering and fail to simulate the effects of inclined strata, which are typically encountered in-situ, on wave propagation.

The complexities associated with the propagation of seismic waves across an inclined layer were assessed using a 2D finite difference analysis program (FLAC 2D v.8.0) [13]. The results highlight the combined action of both P- and S-waves in a soil medium, allowing for the assessment of the conditions that may lead to combined wave loading and the establishment of their relative magnitudes under simpler cases.

Two numerical models were created for this analysis: one with horizontal soil strata and the other with an inclined bedrock having a gentle dip angle of 2.5° . The model has dimensions of 100 m in height and 1000 m in width (aspect ratio of 1:10) and consists of three soil layers: a top soft clay layer of 80 m thick, followed by a 10 m thick glacial till, and bedrock. This reflects the soil profile found in some regions of the Ottawa valley.

The soil is modeled using an elastic model with hysteretic damping to account for non-linear behavior, including progressive stiffness degradation and increase in damping with cyclic loading. The unit weight and shear wave velocity (V_s) of soil and bedrock used in this study are shown in Figure 3. The variation of V_s with depth for the top soft clay layer was adopted from [14]. The modulus reduction (G/G_{max}) and damping (ξ) curves are implemented as a continuous function in the FLAC hysteresis model. The G/G_{max} and ξ curves from [15] for clay are used for the analysis.

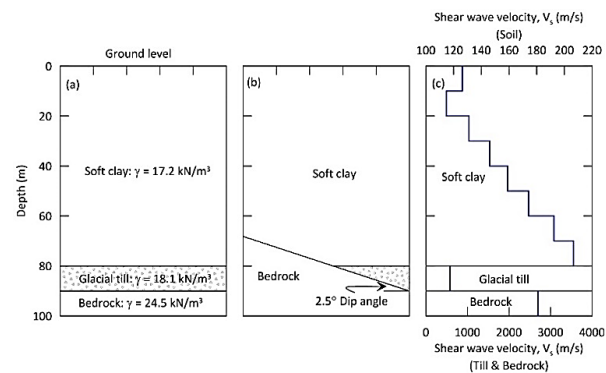


Figure 3: Schematic representation of the developed numerical model (after Prasanna and Sivathayalan 2021 [7])

The grid size of the model is fixed based

on the minimum V_s and frequency content (f) of the input motion. To ensure accurate wave propagation, the element size Δl should be between one-tenth to one-eighth of the wavelength of the highest frequency component of the input motion:

$$\Delta l = 0.1 \left(\frac{V_s}{f} \right) \text{ to } 0.125 \left(\frac{V_s}{f} \right). \quad (4)$$

For a minimum $V_s = 110$ m/s and cutoff frequency $f = 10$ Hz, a minimum Δl of 1.1 m is needed. Hence, a numerical grid of 1000×100 elements with $\Delta l = 1$ m is used here. A quiet viscous boundary is applied at the bottom of the numerical model to absorb the reflected outward propagation waves from the model boundary. Free field boundary conditions are applied at the lateral boundaries to simulate the free field condition. After solving the model for static equilibrium, ground motion analysis is carried out by applying the 1989 Loma Prieta (California) earthquake (PEER strong motion earthquake database, station: 090 CDMG STATION 47381) acceleration at the base of the numerical model. The peak ground acceleration (PGA) of the Loma Prieta EQ ground motion is 0.367 g.

To validate the developed numerical model, results from a 2D horizontal layer model are compared with those obtained from equivalent-linear SHAKE [16] analysis implemented in the GUI program ProShake. The details of model validation are presented in [7]. Figure 4 shows the horizontal and vertical surface acceleration at the midpoint of both horizontal and inclined bedrock models under Loma Prieta EQ ground motion.

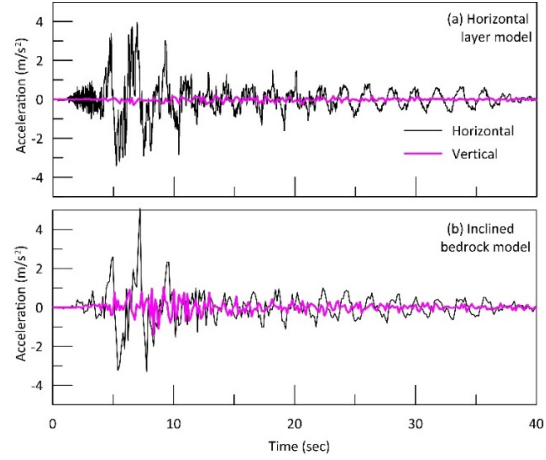


Figure 4: Horizontal and vertical surface acceleration at midpoint of (a) horizontal layer model (b) inclined bedrock

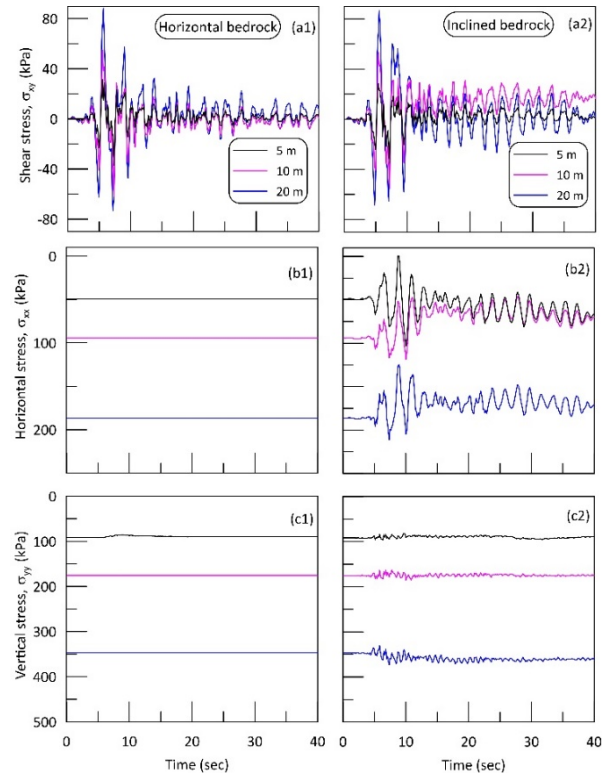


Figure 5: Variation of normal and shear stresses for Loma Prieta ground motion

It can be observed that there is no notable vertical acceleration in the horizontal model,

whereas the inclined bedrock model shows a peak vertical acceleration of 0.17 g. This clearly demonstrates that even a slight deviation from the horizontal can generate both compression (P-waves) and shear waves (S-waves) in the soil during earthquake loading. The P-wave gives rise to normal stresses, whereas the S-wave gives rise to shear stresses in the soil element.

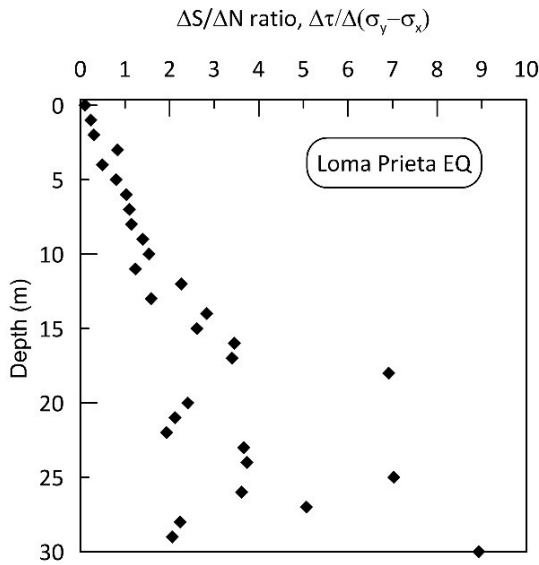


Figure 6: Variation of $\Delta S/\Delta N$ along the centerline of inclined bedrock model

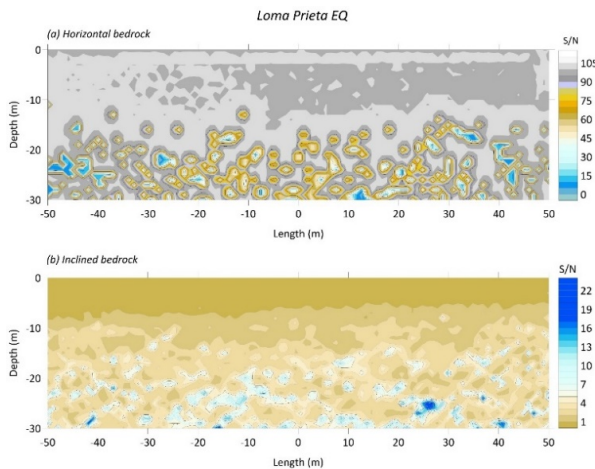


Figure 7: $\Delta S/\Delta N$ contour for Loma Prieta EQ ground motion.

Figure 5 shows the variation of normal and shear stresses at three depths along the centerline of both horizontal and inclined bedrock models. No normal stresses were induced in the horizontal soil strata, while significant normal stresses were observed in the inclined strata due to incoming shear waves. The ratio of peak shear stress to peak normal stress increments

$$\frac{\Delta S}{\Delta N} = \frac{\Delta \tau_h}{\Delta \sigma_v - \Delta \sigma_h} \quad (5)$$

is calculated and plotted at different depths along the midpoint of the model for inclined bedrock model in Figure 6.

Figure 7 presents the variation of $\Delta S/\Delta N$ contours for a 100 m wide and 30 m deep grid. $\Delta S/\Delta N$ is computed along 50 m on either side of the model's centerline, from ground surface to a depth of 30 m. A maximum limit of 100 is set for $\Delta S/\Delta N$ because the value tends to be large at very low normal stresses. The contour shows that $\Delta S/\Delta N$ is mostly 100 for horizontal strata, indicating no normal stresses induced by vertically propagating S-wave. For inclined bedrock strata with a gentle dip of 2.5°, $\Delta S/\Delta N$ ranges from 0.05 to 30. This simulation demonstrates that even a slight dip can result in the simultaneous propagation of P-waves and S-waves.

COMPLEX SEISMIC LOADING PATHS

Conventional CSS and CTX tests cannot simulate the simultaneous action of both compression and shear waves. CSS simulates S-wave loading, while CTX simulates P-wave loading. To simulate complex generalized loading paths, specialized equipment such as a hollow cylinder torsional shear apparatus is

required.

From the numerical investigation presented in the previous section, it is evident that even a slight dip of bedrock can generate both compression and shear waves during a seismic event. Therefore, during earthquake shaking, the soil element is subjected to two components of shear stress: The shear stress on the horizontal plane ($\Delta\tau_h$) due to the S-wave, which is analogous to CSS, and (ii) the shear stress induced due to normal stress increments ($\Delta\sigma_v - \Delta\sigma_h$) on account of the P-wave, which is analogous to CTX loading mode. Here, the complex stress paths resulting from the interaction of seismic waves are evaluated in terms of hollow cylinder terminology. For clarity, $\Delta\tau_h$ is represented as ΔS , and $\Delta\sigma_v - \Delta\sigma_h$ as ΔN herein. Using hollow cylinder torsional shear (HCT) test terminology, $\tau_{z\theta} = \tau_h$ and $\Delta\sigma_z - \Delta\sigma_\theta = \Delta\sigma_v - \Delta\sigma_h$. The ratio $\Delta S/\Delta N$ is intended to be a proxy for the relative magnitude of the stress changes caused by S- and P-waves. Prasanna and Sivathayalan (2021) [7] examined simultaneous P- and S-wave propagation and reported that consolidation stress ratio ($K_c = \sigma'_1 c/\sigma'_3 c$), the ratio $\Delta S/\Delta N$, and phase shift between the waves (δ) significantly influence the nature and degree of stress rotation.

Figure 8 shows different patterns of stress paths in $\tau_{z\theta} - (\sigma_z - \sigma_\theta)/2$ space under varying δ , with $K_c = 1$ and $\Delta S/\Delta N = 0.5$. The stress path is linear when the two stress waves are in phase ($\delta = 0^\circ$), but circular or elliptical when there is a phase shift ($\delta \neq 0^\circ$). The complex nature and degree of stress rotation under this coupled loading condition is also shown in the figure. The elliptical stress path is characterized by a

simultaneous change in both the magnitude of deviatoric stress and rotation of principal stress axes. In contrast, the circular loading path involves continuous rotation of principal stress axes without any change in the magnitude of the deviatoric stress (Figure 8).

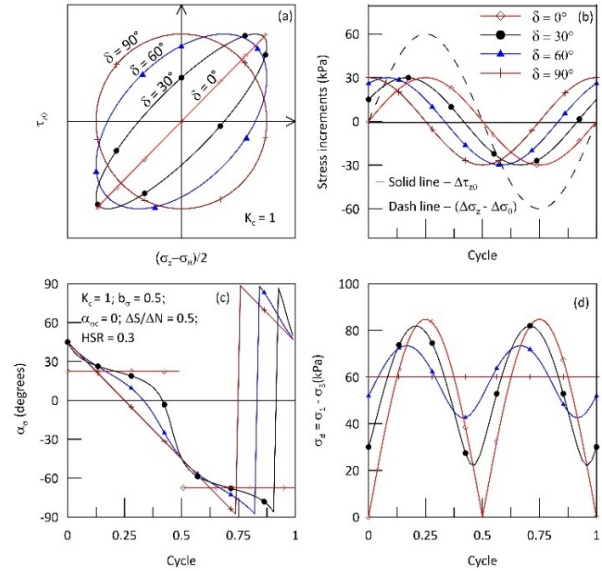


Figure 8: Coupled loading with phase shift between compression and shear waves. (a) Stress path. (b) Variation of shear stress and normal stress increments. (c) Variation of α_σ (d) Variation of σ_d (after Prasanna and Sivathayalan [7])

CYCLIC STRESS RATIO

As discussed previously, the definition of CSR (Cyclic Shear Ratio) is based on the notion of normalized cyclic shear stress intensity. The intensity of cyclic loading is generally defined in terms of simpler, 2D CSS (Cyclic Shear Stress) or CTX (Cyclic Triaxial) stress states ($\frac{\sigma_{d,cy}}{2\sigma'_3 c}$ in triaxial, or $\frac{\tau_{h,cy}}{\sigma'_v c}$ in simple shear) and sometimes in terms of 3D stress states $\frac{\sigma_{d,cy}}{2\sigma'_{m,c}}$. The maximum value of the intensity of the cyclic loading is then termed the CSR. This is fairly straightforward if the cyclic loading is

due to the variation of one stress parameter; e.g., typically an imposed $\Delta\sigma_v$ causes $\sigma_{d,cyc}$ under cyclic triaxial loading, and $\Delta\tau_h$ causes the τ_{cy} in simple shear loading. The maximum cyclic stress amplitude is unambiguously defined in these cases. The maximum shear stress, τ_{max} , is equal to $\frac{(\sigma_1 - \sigma_3)}{2}$, and mathematically the sign of τ_{max} stays always positive, since $\sigma_1 > \sigma_3$, where σ_1 and σ_3 are the major and minor principal stresses respectively.

But in triaxial and simple shear tests, it is customary to assign a sign convention for τ_{max} based on the direction of loading. In triaxial tests, the sign of τ_{max} is taken as positive when $\sigma_v > \sigma_h$, and it is considered negative when $\sigma_h > \sigma_v$ whereas in simple shear, τ_{max} takes the sign of the applied τ_h . Hence, with the sign convention, τ_{max} varies continuously in a smooth sinusoidal manner, which makes the definition of CSR straightforward in these tests. Figure 9 shows the typical variation of CSR in both triaxial and simple shear tests under different initial conditions. In practice, the maximum amplitude from the initial state or (maximum-minimum)/2 is usually defined as CSR (Ishihara 1996) as depicted in Figure 9.

In CHC (Conventional Hardening Criteria), CSR can be defined as the ratio of τ_{max} to the effective mean normal stress ($CSR_{HC2D} = \frac{\tau_{max}}{\sigma'_m c}$) in a manner consistent with CTX and CSS, or as the ratio of octahedral shear stress to the mean normal stress ($CSR_{HC3D} = \frac{\sqrt{3J_2}}{\sigma'_m c}$). The latter formulation considers the 3D stress state (or the intermediate principal stress in addition to major and minor) and is related to the 2D formulation [3] using the b_σ parameter as:

$$CSR_{HC3D} = 2CSR_{HC2D} \sqrt{1 - b_\sigma + b_\sigma^2}$$

The assignment of the sign convention to τ_{max} will be quite straightforward in HCT (High Cyclic Testing) if the cyclic loading is unidimensional, i.e., it is due to changes in either torsional shear stress or axial normal stress. However, this becomes complicated if the loading is multidimensional, involving simultaneous changes in both torsional shear stress and axial normal stress. But this will get complicated, if the loading is multidimensional involving simultaneous changes in both torsional shear stress, and axial normal stress. Such a coupling of both normal and shear stresses can lead to complex cyclic waveforms.

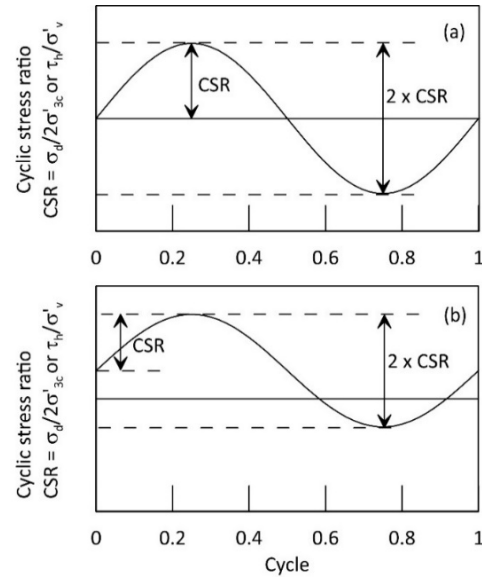


Figure 9: Variation of cyclic loading intensity (a) with no initial static shear, and, (b) with static shear stress.

When an isotropically consolidated (IC) soil element is subjected to coupled loading with waves being in phase with each other, τ_{max} can be assigned the sign of either $\tau_{z\theta}$ or $(\sigma_z - \sigma_\theta)$, since both $\tau_{z\theta}$ and $(\sigma_z - \sigma_\theta)$ change sign at the same time. Assigning a sign convention for

τ_{\max} requires careful consideration in the case of more complex loading, such as ($K_c = 1; \delta \neq 0^\circ$); ($K_c \neq 1; \delta = 0^\circ$) and ($K_c \neq 1; \delta \neq 0^\circ$).

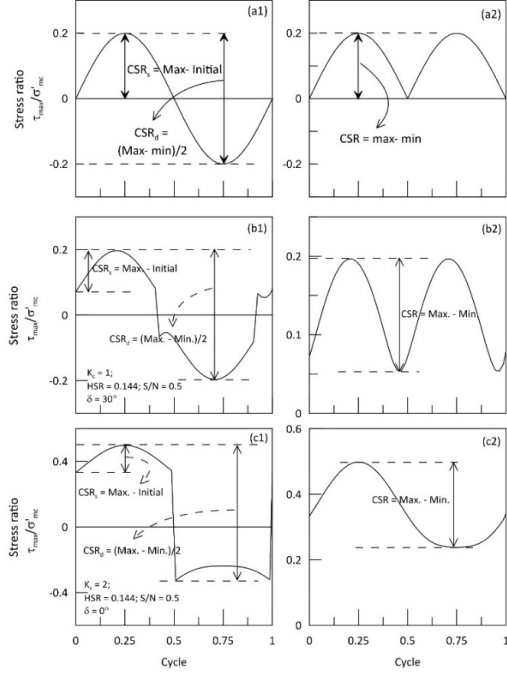


Figure 10: Variation of cyclic loading intensity under generalized loading conditions.

Figure 10 shows the definition of CSR based on two cases: (a) if τ_{\max} follows the sign convention of $\tau_{z\theta}$, and (b) the sign-independent nature of τ_{\max} (since $\sigma_1 > \sigma_3$). It can be observed that with the sign convention, the CSR variation is not continuous and is not symmetrical for some cases. In these cases, CSR can be defined in two possible ways, i.e., single amplitude-based CSR ($CSR_s = \text{maximum} - \text{initial value}$), or double amplitude-based CSR ($CSR_d = (\text{maximum} - \text{minimum})/2$) as shown in Figure 10 (a1, b1, and c1). On the other hand, with sign independence, the CSR variation is smooth and continuous, and it is defined as the difference between the maximum and minimum values (Figure 10 (a2, b2, and c2)). The CSR_d with sign convention

can be treated as equivalent to CSR (maximum - minimum) with sign independence as depicted in Figure 10 (a1 and a2).

Nomenclature

1. α_σ :- Inclination of major principal stress axis with respect to vertical axis of deposition, $\tan^{-1} \left(\frac{\tau_{z\theta}}{\sigma_z - \sigma_3} \right)$
2. δ :- Phase shift between the cyclic normal and shear stresses
3. $\sigma_z, \sigma_r, \sigma_\theta$:- Axial, radial, and circumferential stress
4. $\sigma'_1, \sigma'_2, \sigma'_3$:- Effective major, intermediate, and minor principal stress (*Subscript c indicates values at the end of consolidation*)
5. σ'_m :- $\frac{\sigma'_1 + \sigma'_2 + \sigma'_3}{3}$, Effective mean normal stress
6. σ_d :- $\sigma_1 - \sigma_3$, Deviatoric stress
7. σ'_{vo} :- Effective vertical overburden stress
8. $\tau_{(cy,max)}$:- Maximum cyclic shear stress
9. b_σ :- $\frac{\sigma_2 - \sigma_3}{\sigma_1 - \sigma_3}$, Intermediate principal stress parameter
10. K_c :- Principal stress ratio, $\frac{\sigma'_{1c}}{\sigma'_{3c}}$
11. CSR :- Cyclic stress ratio
12. CRR :- Cyclic resistance ratio
13. $\sigma_{d,cy}$:- Cyclic deviatoric stress
14. G and ξ :- Shear modulus and damping ratio

Summary & Conclusions

Seismic wave propagation analysis shows that soils elements in-situ could be subjected to both cyclic normal and shear stress changes

during earthquakes. This is especially the case if the soil strata at the site is inclined, even by a couple of degrees. Such loading cannot be simulated by cyclic triaxial or cyclic simple shear tests and can only be simulated using a cyclic torsional shear test. The variation in the cyclic waveform can be complex under such simultaneous loading, and the traditional definitions of CSR cannot be used to properly represent the cyclic loading intensity. These difficulties arise due the 2D centric approach to cyclic liquefaction, and they might be avoided by using the 3D stress state, or stress invariants to define the CSR. However, the use of stress invariants would not permit characterization of direction dependent response.

References

- [1] Youd, T.L., Idriss, I.M., Andrus, R.D., Arango, I., Castro, G., Christian, J.T., Dobry, R., Finn, W.D.L., Harder Jr, L.F., Hynes, M.E., Ishihara, K., Koester, J.P., Liao, S.C., Marcuson III, W.F., Martin, G.R., Mitchell, J.K., Moriwaki, Y., Power, M.S., Robertson, P.K., Seed, R.B., and Stokoe II, K.H. 2001. Liquefaction Resistance of Soils: Summary Report from the 1996 NCEER and 1998 NCEER/NSF Workshops on Evaluation of Liquefaction Resistance of Soils, *Journal of Geotechnical and Geoenvironmental Engineering*, 127(10): 817- 833.
- [2] Seed, H. B. (1983). "Earthquake-resistant design of earth dams." Proc., Symp. Seismic Des. of Earth Dams and Caverns, ASCE, New York, 41-64.
- [3] Prasanna, R and Sivathayalan, S. (2024). "Liquefaction characteristics of sand under complex seismic loading paths".*Journal of Geotechnical and Geoenvironmental Engineering*, ASCE (In-Press).
- [4] Tastan, E. O., and Carraro, H. A. J. (2022). "Effect of Principal Stress Rotation and Intermediate Principal Stress Changes on the Liquefaction Resistance and Undrained Cyclic Response of Ottawa Sand." *Journal of Geotechnical and Geoenvironmental Engineering*, 148(5), 04022015.
- [5] Sivathayalan, S., 2011, Review of initial state and stress path effects on liquefaction resistance of sands, In Proc. Geotechnical Engineering For Disaster Mitigation And Rehabilitation And Highway Engineering. pp. 197-207.
- [6] Sivathayalan, S., and Vaid, Y. P. (2002). "Influence of generalized initial state and principal stress rotation on the undrained response of sands".*Canadian Geotechnical Journal*, 39(1), 63-76.
- [7] Prasanna, R ., and Sivathayalan, S. (2021). "A Hollow Cylinder Torsional Shear Device to Explore Behavior of Soils Subjected to Complex Rotation of Principal Stresses", *Geotechnical Testing Journal* , 44(6), 1595-1616.
- [8] Idriss, I.M., and Boulanger, R.W. (2008). "Soil liquefaction during earthquakes", Monograph MNO-12, Earthquake Engineering Research Institute, California.
- [9] Ishihara, K., Iwamoto, S., Yasuda, S., and Takatsu, H., (1977). Liquefaction

- of anisotropically consolidated sand, in Proceedings, 9th International Conference on Soil Mechanics and Foundation Engineering, Japanese Society of Soil Mechanics and Foundation Engineering, Tokyo, Japan 2, pp. 261-64.
- [10] Ishihara, K, Yamazaki, A, and Haga, K., (1985). Liquefaction of Ko consolidated sand under cyclic rotation of principal stress direction with lateral constraint, Soils and Foundations, Japanese Society of Soil Mechanics and Foundation Engineering 5(4), 63-74.
- [11] Pyke, R. M., Chan, C. K., and Seed, H. B., (1974). Settlement and Liquefaction of Sands under Multi-Directional Shaking, Report No. EERC 74-2, Earthquake Engineering Research Center, University of California at Berkeley.
- [12] Prasanna, R and Sivathayalan, S. (2022). "Liquefaction of sands subjected to principal stress rotation caused by generalized seismic loading". Canadian Geotechnical Journal, 59(8), 1427-1442 <https://doi.org/10.1139/cgj-2021-0035>.
- [13] Itasca Consulting Group. (2016). FLAC - Fast Lagrangian Analysis of Continua - dynamic analysis, FLAC Version 8. Minneapolis, Itasca.
- [14] Kasgin, K. B., (2010). "Site Response Analysis and Seismic Surveying of High Contrast Soil Profiles for the City of Ottawa" Ph.D thesis, Carleton University.
- [15] Sun, L., Gu, C., and Wang, P. (2015). "Effects of cyclic confining pressure on the deformation characteristics of natural soft clay." *Soil Dynamics and Earthquake Engineering*, Elsevier, 78, 99-109.
- [16] Schnabel, P.B., Lysmer, J. & Seed, H.B., (1972). "SHAKE: a computer program for earthquake response analysis of horizontally layered sites" Report EERC-71-12, University of California, Berkeley: Earthquake Engineering Research Center (EERC).